



**Characterization, fate and transport of floc aggregates in  
full-scale flocculation tanks**

|                               |   |
|-------------------------------|---|
| Journal:                      | <i>Environmental Science: Water Research &amp; Technology</i>   |
| Manuscript ID                 | EW-ART-11-2015-000259.R1  |
| Article Type:                 | Paper   |
| Date Submitted by the Author: | 11-Dec-2015   |
| Complete List of Authors:     | Gagnon, Graham; Dalhousie University, Civil and Resource Engineering<br>Vadasarukkai, Yamuna; Dalhousie University, Civil and Resource<br>Engineering |
|                               |   |

# 1 **Characterization, fate and transport of floc aggregates in full-scale flocculation tanks**

2 Yamuna S. Vadasarukkai\* and Graham A. Gagnon\*<sup>§</sup>

3 \* Department of Civil and Resource Engineering, Dalhousie University, Canada

4 <sup>§</sup>Corresponding Author: Dr. G.A. Gagnon, Dalhousie University, Halifax, NS, B3J 1Z1,  
5 e-mail: [graham.gagnon@dal.ca](mailto:graham.gagnon@dal.ca), Tel: 902.494.3268, Fax 902.494.3108

## 6 **1. Abstract**

7 Floc size distribution is of high operational importance as it governs the transport and  
8 removal of contaminants from drinking water. The complex nature of turbulent flow in treatment  
9 plants has limited the research to quantify the dynamics of flocculation. This paper describes the  
10 use of a submersible digital in-line holographic microscopy (DIHM) technique for the  
11 measurement of the spatial distribution of floc sizes in a direct filtration treatment facility. The  
12 DIHM tool was positioned at thirteen different locations in a flocculation tank and holograms  
13 were recorded for at least 10 minutes at each location. The acquisition of morphological details  
14 of flocs (e.g., floc counts, size distributions and floc velocities relative to the fluid motion) from  
15 the reconstructed DIHM images is discussed. The results of the spatial distribution of floc sizes  
16 indicated that the volume equivalent floc diameter measured in the flocculation tank was mostly  
17 of large-sized aggregates greater than 100  $\mu\text{m}$ , which can have adverse impacts on the  
18 performance of a direct filtration process. The relative motion of flocs calculated from the DIHM  
19 analysis ranged from 0.002 to 0.008 m/s. Results showed that the investigated DIHM technique  
20 could be used as an operational tool to evaluate flocculation performance in terms of floc sizes,  
21 which is otherwise difficult to characterize in most treatment plants. The information acquired  
22 from this tool is important to understand the fate and transport of flocs during flocculation for  
23 process optimization that can lead to minimize chemical and energy usage in treatment plants.

## 24 **2. Water impact**

25 The ability to obtain details on floc morphology from in-line measurements will  
26 significantly advance our understanding of the fate and transport of flocs with their associated  
27 contaminants in treatment plants. In this study floc counts, floc size distributions, and floc  
28 velocities are characterized relative to hydrodynamics in a hydraulic flocculation tank. The  
29 results demonstrated that large, irregular shaped floc aggregates were formed in flocculation due  
30 to limited supply of active mixing in the tank. Accumulation of large flocs on filters has an

31 economical impact on the plant performance. In a broader context, the ability to understand floc  
32 formation in real-time has potential to assist in other environmental applications (e.g.,  
33 wastewater treatment, algal detection).

### 34 **3. Introduction**

35 Coagulation is an important treatment process for the removal of mineral and organic  
36 particles in water supplies that are typically stable in water.<sup>1</sup> Inorganic metal salts added in  
37 coagulation causes a change to the surface chemistry of constituent particles in source water  
38 mainly by charge neutralization or enmeshment of particles within metal hydroxide precipitates.<sup>2</sup>  
39 Flocculation that follows coagulation is the gentle mixing phase used to achieve contact between  
40 unstable particles in suspension, promoting their aggregation.<sup>3</sup> Particles grow in flocculation  
41 often leading to aggregates of highly porous, loosely connected, irregular shaped structures,  
42 described as flocs.<sup>3,4</sup> High molecular weight polymers are at times added as a flocculant aid to  
43 increase floc strength and size by adsorption and interparticle bridging mechanisms.<sup>5</sup>

44  
45 Flocs represent a complex matrix of microbial communities, colloids and suspended  
46 materials, and organic and inorganic constituents.<sup>6</sup> The size and strength of the developed flocs  
47 determines the efficiency of solids removal processes. Preferred floc characteristics differ  
48 depending on the solids removal processes used-for instance, relatively small, dense and low-  
49 volume flocs are recommended for direct filtration (i.e., no sedimentation step) in order to  
50 enhance the effective use of the media depth.<sup>8</sup> In contrast, large and dense aggregates with high  
51 resistance to breakage are preferred for sedimentation.<sup>9</sup> Although the porosity of aggregates  
52 often increases with floc size, which affects their settling rates, their volume, and dewatering  
53 characteristics of the sludge.<sup>10</sup> Therefore a compromise between sedimentation efficiency and  
54 sludge filtration characteristics has to be achieved in industrial practice.

55  
56 Flocculation is a dynamically active process which is directly influenced by its  
57 hydrodynamic conditions.<sup>9,11</sup> The flow conditions are driven by localized fluid turbulence that  
58 depends on both the geometry of the flocculation tank and the impeller speed and type.<sup>12</sup> Flocs  
59 are transported between zones of varying levels of energy dissipation in a turbulent flow; this  
60 results in a continuous process of aggregation and breakage of flocs.<sup>11</sup> Hopkins and Ducoste<sup>13</sup>

61 showed that the average floc size varied spatially in a flocculation reactor at low mixing speeds  
62 with larger flocs sizes and growth rates in the bulk region and a larger variance in the impeller  
63 discharge region. A simulation study by Samaras et al.<sup>14</sup> showed no large flocs in the region  
64 close to the impeller and floc growth in regions of high residence time. Data on spatial variations  
65 in floc size distribution is an important parameter to understand the transport and removal of  
66 particles in flocculation, sedimentation and filtration of suspensions.<sup>15</sup>

67

68 Measuring floc physical characteristics (e.g. size and morphology) can be achieved by  
69 using a number of different techniques such as optical microscopy<sup>16</sup>, automated image analysis  
70 system<sup>17</sup>, coulter counters<sup>18</sup>, laser diffraction techniques<sup>19</sup>, and photometric dispersion  
71 analyzer<sup>20</sup>. Most of these techniques (including microscopy, imaging analysis, and laser  
72 diffraction) require withdrawal of floc samples through pipetting or pumping and/or dilution of  
73 floc samples prior to the measurement. Such sampling procedures can disrupt the floc structure,  
74 causing floc breakage.<sup>21</sup> In-line methods are advantageous for floc analysis as it eliminates  
75 sample collection and/ preparation issues. Only few studies have used in-line techniques (e.g.,  
76 Oliveira et al.<sup>22</sup>, Chakraborti et al.<sup>23</sup>)- for instance, Chakraborti et al.<sup>23</sup> used a non-intrusive  
77 photographic technique coupled with a digital image processing system to characterize alum floc  
78 aggregates formed in a jar test. But all these aforementioned techniques are limited to laboratory  
79 workbench only.

80

81 Holographic microscopy is a technique that can be used for the characterization of marine  
82 particulates and tracking particle motion, such as the swimming behaviour of microscopic  
83 organisms<sup>24</sup>, and spatial distribution of micrometer and sub-micrometer particles in dense liquid  
84 suspensions.<sup>25</sup> In the current study, a submersible digital in-line holographic microscopy (DIHM)  
85 was used for the non-destructive, direct measurement of floc characteristics (e.g., floc counts,  
86 sizes, relative floc velocities) in a three-stage hydraulic flocculation tank at the J.D. Kline Water  
87 Supply Plant in Halifax, Canada. The flow characteristics of the flocculation tank were  
88 previously modelled using computational fluid dynamics (CFD), as described by Vadasarukkai  
89 et al.<sup>12</sup>. In the previous study, the predicted average velocity gradient (i.e., the G- values) ranged  
90 from 2 to 40 s<sup>-1</sup> at various inflow conditions in the flocculation tank, which was significantly  
91 below the recommended design criteria of 20 to 75 s<sup>-1</sup>.<sup>8</sup>

92

93           The purpose of the current study was to obtain in-line measurements of floc size  
94 distributions and floc velocities relative to the prevailing turbulent flow in hydraulic flocculation  
95 tanks. The potential implications of identified floc characters on filter performance are also  
96 discussed. It was hypothesized that the use of DIHM tool will improve the understanding of flocs  
97 transport in flocculation as it is capable of counting particles, conducting image analysis and  
98 tracking particle motion. The present study is its first application to the authors' knowledge in  
99 the drinking water industry.

#### 100 **4. Materials and methods**

##### 101 **Overview of the study site:**

102           The study was carried out at the J.D. Kline Water Supply Plant in Halifax, Canada. The  
103 design capacity of the plant is about 220 ML/d, with an average daily intake of 95 ML/d. Raw  
104 water is pumped into the direct filtration facility through a 1.2 m (48") inlet pipe, and flows  
105 under gravity into the subsequent treatment processes. As seen in Fig. 1, the treatment process  
106 consists of three rapid mix tanks in series, four parallel units of a three-stage tapered hydraulic  
107 flocculation tanks, eight direct dual-media filtration units in parallel, and chlorination. Calcium  
108 hydroxide (lime) is added for pH adjustment in the first of three premix tanks. Water then passes  
109 to the second premix tank, where additional mixing takes place, and then to the final premix tank  
110 where carbon dioxide is used to adjust to the coagulation pH of 5.5–6 and an average alum dose  
111 of 8 mg/L of aluminum sulfates is added for coagulation.<sup>26</sup>

112

113           Flow distributes the water after coagulation into four identical hydraulic flocculation  
114 tanks. Each flocculation tank contains three rows of two parallel sets of chambers (i.e., total six).  
115 The inlet pipe is located primarily below grade at the site, which divides the incoming water into  
116 the first set of chambers (Fig. 1). The length, width, and depth of each flocculation chamber are  
117 5.0 m, 5.0 m, and 8.3 m, respectively. Two tapered vertical shafts are provided for the water to  
118 transfer between the three rows of flocculation chambers. Each shaft has a capacity of 11.95 m<sup>3</sup>  
119 and 18.68 m<sup>3</sup> respectively. The water enters at an inclined angle into the first chamber due to the  
120 inlet design. After mixing in the first chamber it flows over a weir, then through a vertical shaft,  
121 and enters the next cell from the bottom. The design of an up-and-down flow arrangement in the

122 subsequent second and third flocculation chambers provides the tapered G-value for mixing  
123 purposes.<sup>12</sup> After the flocculation process, the water is distributed to filter units through a floc  
124 water conduit.

#### 125 **DIHM set-up and acquisition of images:**

126 Fig. 2 shows the main components of the submersible digital in-line holographic  
127 microscopy (4deep Inwater Imaging, Halifax, Canada). It consists of a laser source that directs  
128 the light ( $\lambda = 365$  nm) through a 500 nm pinhole. A spherical wave emanates through the pinhole,  
129 which acts as the point source. As seen in the schematic in Fig. 2, it has two pressure chambers,  
130 one of which houses the laser and the other has a CCD camera (JAI PULNIX Inc., Sunnyvale,  
131 CA) connected to a computer source and a power supply. A 3 mm sampling space was provided  
132 between the two chambers to allow free circulation of water (medium) between them. The  
133 sampling space can be adjusted up to an 8 mm range depending on floc sizes to measure.  
134 Interference between the reference wave with a known phase distribution and light scattered  
135 from various size range of floc aggregates in the water was recorded as holograms.<sup>25</sup> The records  
136 of interference patterns contain spatial information about flocs within the imaged volume.

137

138 The present study was conducted on one parallel set of chambers of a hydraulic  
139 flocculation tank. The flow characteristics predicted in the previous CFD study<sup>12</sup> were used to  
140 select different sampling locations to position the submersible microscope in the tank. According  
141 to the model, three distinct regions were identified in the tank – namely, short circuiting,  
142 recirculation and stagnant (non-mixing) zones as shown in Fig. 3. The short circuiting path was  
143 created by a jet velocity of flow near the inlet which caused some portion of the incoming flow  
144 to rapidly exit into the second flocculation chamber. An intense recirculation region was formed  
145 at the interior of the first flocculation chamber, where 10.4% of simulated particles were shown  
146 trapped in that region for a longer residence time from the particle tracking analysis.<sup>12</sup> Stagnant  
147 (or non-mixing) zones depicted in Fig. 3 represented those regions in the second and third  
148 flocculation chambers where the flow path of particles never visited.

149

150 As illustrated in Fig. 4, the DIHM tool was positioned at thirteen different sampling  
151 locations in the flocculation tank to acquire a true representation of the spatial distribution of floc  
152 sizes in a turbulent flow. Specifically, eleven locations in section X-X in the first chamber and

153 two locations in section Y-Y in the last chamber were chosen. These locations were selected  
154 based on the three regions identified from the flow characteristics described previously. For  
155 instance, 1B and 2B were the locations that represented the short circuiting path near the inlet in  
156 the first tank; locations 4M and 4B at the center denoted the recirculation region. No sampling  
157 location was selected for the second flocculation chamber as the fluid velocity was low in the  
158 stagnant zones (Fig. 3). Only two locations, 6T and 6B, were selected for the last (third)  
159 flocculation chamber, where location 6T was situated near the peripheral outflow.

160

161 At each selected location, the DIHM was placed perpendicular to the fluid motion to  
162 allow free circulation of water through the sampling space. The instrument was held firmly using  
163 a rope, and the holograms were recorded continuously for 10 minutes at 15 fps by the CCD  
164 camera as illustrated in Fig. 5. Data was transmitted from the camera to the computer via an  
165 underwater cable. All the recorded holograms were stored as bitwise digital images in the  
166 computer for further analysis.

#### 167 **Image processing- hologram reconstruction and measuring the floc aggregates:**

168 Stored holograms were reconstructed numerically to obtain images of floc aggregates  
169 within the imaged volume. Software (Holosuite, 4deep Inwater Imaging) was used to reconstruct  
170 each batch of holograms acquired at a sampling location. An example of reconstruction step is  
171 illustrated in Fig. 6. Here, two consecutive holograms were paired to remove the background  
172 noise. This combined file, called the difference hologram, was then reconstructed with the  
173 Kirchhoff-Helmholtz transform<sup>27</sup> to obtain images at a particular depth plane in the sample  
174 volume.

175

176 The morphological details of flocs, including floc counts and size distribution, were  
177 processed from the reconstructed DIHM images. The pixel value of the image was enhanced  
178 using the threshold tool to detect the floc aggregates from the background noise. Typically, the  
179 pixel value varied between 0 and 255, where 0 was considered as black and 255 signified the  
180 white color. Those images with pixel values greater than the adjustable threshold value were  
181 recognized as “floc aggregates”; the rest of the image was inferred as background pixels, as  
182 suggested by Wu et al., 2010. The threshold value of the original image was adjusted between  
183 110 and 120% by manually examining it for at least 5-10 reconstructed images. The dilation and

184 erosion factors were used to enhance the identified flocs. It was seen that a 10- 12 of dilation and  
 185 1-3 of erosion were the best suitable values for measuring flocs. The entire sequence of  
 186 reconstructed DIHM images was then automatically counted, based on the parameter values that  
 187 were manually adjusted for the first image.

188

189 Eq. (1) was used to measure the equivalent circular diameter,  $d$  ( $\mu\text{m}$ ), from the projected  
 190 area ( $A$  in  $\mu\text{m}^2$ ) of a floc detected using the DIHM analysis. The volume and mass distribution of  
 191 flocs is important for the control of floc sizes in solid-liquid separation process. Thus, floc size  
 192 distribution was expressed as the volume fraction of floc diameter in each bin using Eq. (2).

$$193 \quad d = \sqrt{\frac{4A}{\pi}} \quad (1)$$

$$194 \quad dV_i = \frac{\left(\frac{\pi d_i^3}{6}\right) * \left(\frac{dN_i}{N}\right)}{V} \quad (2)$$

195 Here,  $dV_i$  is the volume fraction of flocs in the  $i^{\text{th}}$  class interval, the term  $\left(\frac{\pi d_i^3}{6}\right)$  is the

196 average volume of flocs in the  $i^{\text{th}}$  class interval by assuming flocs are spherical, the term  $\left(\frac{dN_i}{N}\right)$

197 is the frequency of occurrence for the  $i^{\text{th}}$  class interval with  $dN_i$  number of flocs,  $V$  is the total  
 198 floc volume.

### 199 **Floc velocity measurements:**

200 Floc velocity was calculated by overlaying two subsequent holograms. Overlaying the  
 201 reconstructed holograms highlighted only the floc motion relative to the fluid (water) velocity,  
 202 while the rest of the stationary features were deducted during this process. The distance travelled  
 203 was manually measured (Fig. 7). The relative magnitude of velocity of a floc was calculated as  
 204 the ratio of distance travelled and the time between frames. Nearly, 30-50 flocs were tracked to  
 205 obtain a statistically significant velocity magnitude profile. It was challenging to track flocs, and  
 206 to calculate their velocities at locations that had minimum fluid velocity (e.g., stagnant zones).

## 207 5. Results of full-scale data

### 208 **Floc size distribution:**

209 The floc size distribution was evaluated for the thirteen locations in the flocculation tank.  
210 Fig. 8 illustrates the volume-based floc equivalent diameter measured at one such sampling  
211 location (1B in the first flocculation chamber). The value of the median equivalent diameter was  
212 188  $\mu\text{m}$  at this location, with a 90<sup>th</sup> percentile of 300  $\mu\text{m}$ . Similar information about the floc size  
213 distribution was acquired from the data collected at the remaining locations (1M to 6B). Box and  
214 whisker plots were used to demonstrate spatial variations in the equivalent floc diameter as  
215 shown in Fig. 9 (A) and (B). In Fig. 9 (A), the data in the section X-X was arranged into four  
216 groups (A, B, C and D) with reference to the flow trajectory. Most distributions were positively  
217 skewed, with the median equivalent floc diameter varying from 175 to 225  $\mu\text{m}$  at these locations.  
218 A log-normal distribution ( $\alpha=0.01$ ) was a suitable fit for the size distribution of floc aggregates,  
219 the finding which is in agreement with earlier studies.<sup>18</sup> Although five sampling locations (i.e.,  
220 1B, 2M, 5B, 5M, and 5T) did not fit any of the models tested, including Weibull, log-normal,  
221 exponential, and gamma distributions.

222  
223 Levene's test ( $\alpha=0.05$ ;  $N > 16$ ) was used to assess the variation in floc size distribution  
224 within each group; it showed no significant difference in floc aggregate sizes formed in the  
225 section X-X, except for locations in Group B (i.e., 2T, 2M and 2B). The spatial distribution of  
226 floc size was related to the local velocity of the fluid phase, and the turbulent energy dissipation,  
227 as described in previous studies.<sup>14, 28, 29</sup> A detailed description of the predicted velocity  
228 distribution for the sections X-X and Y-Y is illustrated in Fig. A (1) in the supplementary  
229 information. Initially, flocs followed the trajectory of the main inlet flow stream, which was the  
230 main source of mixing intensity for flocs to interact in the hydraulic flocculation tank. The actual  
231 floc growth was observed more towards the upper middle and top portions of the tank. A few  
232 floc aggregates of larger than 550  $\mu\text{m}$  in diameter, identified as outliers in Fig. 9 (A), were  
233 prominent in Group A (i.e., 1T, 1M and 1B) and Groups B (i.e., 2T, 2M and 2T). 3M and 4M,  
234 situated at the interior of the flocculation tank, had a narrow distribution of floc aggregates with  
235 median values between 175 and 200  $\mu\text{m}$ . In these recirculation zones, lower velocities (0 to  
236 0.015 m/s) were observed, causing fewer particle interaction(s) and limiting floc size.

237

238 In the last flocculation chamber, a broader distribution of floc sizes ranging from 100 to  
239 750  $\mu\text{m}$  was observed, as shown in Fig. 9 (B). This resulted in a heterogeneous floc suspension  
240 near the peripheral outflow, with 95% percent of the volume fraction of floc sizes less than or  
241 equal to 674  $\mu\text{m}$ .

#### 242 **Measurements of relative velocity of floc aggregates:**

243 The relative motion of individual floc aggregate with respect to the fluid motion was  
244 tracked using the recorded holograms. As shown in Fig. 10, median values of the relative  
245 velocity of flocs varied significantly from 0.003 to 0.009 m/s at each location. A jet inflow  
246 velocity of approximately 0.1-0.16 m/s near the entrance caused flocs at 1B, 2B and 5B locations  
247 to experience a relative floc velocity of up to 0.016 m/s, following the trajectory of the fluid  
248 motion. The sampling locations 5B, 5M and 5T in Group D had a clear trend of decreasing  
249 values of median floc velocities from 0.007 to 0.004 m/s along the depth. This suggested the  
250 upward flow of water to the rest of the tank appeared to reduce the floc velocity at the middle  
251 and top locations. But, this trend was not consistent in the sampling locations of Group A and B,  
252 which were situated in a high velocity profile location with the local velocity magnitude ranging  
253 between 0.03 and 0.08 m/s. These locations (1T, 1M, 1B, 2T, 2M and 2B) had median floc  
254 velocities ranging between 0.006 and 0.008 m/s. The low fluid velocity profile of less than 0.015  
255 m/s in the recirculation regions (3M and 4M) had the interquartile relative floc velocities ranging  
256 from 0.005 to 0.006 m/s.

257  
258 The relative motion of flocs calculated from the DIHM analysis was in reasonable  
259 agreement with the fluid flow. At large, the predicted fluid velocities (0.02 to 0.055 m/s) from  
260 the CFD analysis were approximately an order of magnitude larger than the DIHM calculated  
261 particle velocity (0.002 to 0.008 m/s). The variation in the average relative velocity of flocs to  
262 the fluid motion is attributable to two possible reasons- (i) the actual plant flow was 86.72 ML/d  
263 at the time of floc analysis, which was less than the modelled flow rate of 90 MLD (ii) floc  
264 velocities were tracked for a wide range of flocs sizes from 20 to over 500  $\mu\text{m}$  measured in the  
265 flocculation chamber. Saffman and Turner<sup>30</sup> found that small agglomerates (<15  $\mu\text{m}$ ) in water  
266 treatment plants follow the fluid motion completely. The larger floc sizes predominantly found in  
267 the flocculation tank exhibited inertia with respect to turbulent flow fluctuations leading to a  
268 motion of particles different from that of the fluid, as suggested in Abrahamson's<sup>31</sup> work.

## 269 6. Practical implications

270 The DIHM analysis demonstrated a relatively quiescent condition in the flocculation  
271 process, which was in agreement with the earlier CFD findings.<sup>12</sup> Flocs formed in the hydraulic  
272 flocculation tank received a limited supply of active mixing in the chambers, aside from the inlet  
273 and small openings in weir columns between the chambers. Median floc sizes of 200-225  $\mu\text{m}$   
274 were formed in the regions that had the local velocity range of 0.035 to 0.07 m/s. Flocs that were  
275 entrained in the recirculation region in locations 3M and 4M of high residence time<sup>12</sup> had a  
276 narrow distribution of floc aggregates. These regions are recognized to contribute less to floc  
277 sizes in the peripheral outflow and are thus less connected to the solid-liquid separation  
278 processes (e.g., sedimentation, filtration).<sup>14</sup> Approximately 25% of volume fractions of floc sizes  
279 measured near the outflow in the present study was larger than 500  $\mu\text{m}$ . As a consequence, bulky  
280 and irregular shaped floc aggregates represented the overall floc morphology in the hydraulic  
281 flocculation tank.

282  
283 In direct filtration, as the entire solid-liquid separation takes place in the filter itself, the  
284 floc size is an important operational parameter.<sup>32</sup> Filter beds in direct filtration processes are  
285 designed with a large floc holding capacity<sup>8</sup> that can retain a considerable volume of floc sizes  
286 larger than the effective filter pore size. Alternatively, fine flocs sizes of the order of 1  $\mu\text{m}$  are  
287 not readily captured by typical filter grains.<sup>33</sup> Their small sizes are more likely to bypass the  
288 filters along with the treated effluent, which can pose potential risks to the drinking water  
289 quality. The volume equivalent floc diameter measured in the flocculation tank was larger than  
290 the optimum sizes recommended in the literature. For instance, the simulation results of Ngo et  
291 al.<sup>32</sup> indicated that a mean floc diameter of 62  $\mu\text{m}$  was the optimal size for direct filtration.  
292 Similar results by Pivokonsky et al.<sup>9</sup> demonstrated that small, highly compact and regular  
293 aggregates of most probable diameter of 50  $\mu\text{m}$  displayed the best filterability. In the present  
294 case, over 98% of the particle count near the peripheral outflow was tied to flocs larger than 100  
295  $\mu\text{m}$ .

296  
297 The open structure of large floc aggregates can have adverse impacts on the performance  
298 of a direct filtration process. Such floc structures are susceptible to breakage during  
299 transportation through the floc tunnel to the filtration unit, potentially leading to filter

300 performance issues such as turbidity breakthrough. Jarvis et al.<sup>19</sup> showed consistent decrease in  
301 floc sizes in three different floc suspensions when exposed to increased rotational speeds, with  
302 little re-growth potential after the breakage. Large floc sizes can also reduce the effective filter  
303 run times in a direct filtration plants. Pivokonsky et al.<sup>9</sup> showed that a high proportion of large  
304 (i.e., 155-1330  $\mu\text{m}$ ) floc aggregates formed during coagulation/flocculation processes caused a  
305 high pressure drop in deep-bed filtration and thereby, significantly shortened filter run time.

## 306 7. Conclusions

307 This study demonstrated the applicability of the submersible digital in-line holographic  
308 microscopy (DIHM) technique for the measurement of the spatial distribution of floc sizes in  
309 full-scale flocculation tanks. The spatial distribution of floc sizes indicated that the volume  
310 equivalent floc diameter measured in the flocculation tank was mostly large-sized aggregates of  
311 greater than 100  $\mu\text{m}$ , which was larger than the optimum floc size ( $\sim 50 \mu\text{m}$ ) recommended for  
312 direct filtration by other studies (e.g., Pivokonsky et al.<sup>9</sup>). In direct filtration, large flocs can  
313 quickly cover the top surface of the filter media, reducing the effective use of the entire media  
314 depth. Practical issues of operating at such conditions in a direct filtration facility are rapid  
315 clogging of filters, resulting in excessive backwashing due to a high rate of head loss  
316 development.

317

318 The performance of a hydraulic flocculation tanks was evaluated using in-line  
319 measurements of floc size distributions, which is otherwise difficult to characterize in treatment  
320 plant with respect to the prevailing turbulent flow. The motion of individual floc aggregate  
321 tracked in the DIHM showed relative velocities ranging from 0.002 to 0.008 m/s. At large, the  
322 velocity magnitude of fluid motion (0.02 to 0.055 m/s) from the CFD predictions was  
323 approximately an order of magnitude larger than the DIHM calculated particle velocity.  
324 Regularly acquiring critical information on the type of flocs formed in flocculation can assist  
325 water utilities to take corrective actions (e.g., adjust coagulant dosage, pH, mixing) to improve  
326 filter performance. The information from this study is important for understanding the fate and  
327 transport of flocs during the flocculation process for process optimization that can lead to  
328 minimize chemical and energy usage in treatment plants. The ability of DIHM to measure  
329 particles sizes and to compute the relative particle velocities is likely to contribute to the

330 advancement of new technologies for the water and wastewater industry in other environmental  
331 applications (e.g., algal, microbial detections).

## 332 8. Acknowledgements

333 The authors acknowledge the support of the Natural Sciences and Engineering Resource Council  
334 of Canada (NSERC) and 4deep Inwater Imaging through an NSERC Engage Grant, as well the  
335 financial support of both NSERC and Halifax Water through the NSERC/Halifax Water  
336 Industrial Research Chair program. The authors also acknowledge the technical and in-kind  
337 support of Dr. Manfred H. Jericho, Stefan Jericho and John Samson from the department of  
338 Physics at Dalhousie University during the initial design and implementation phase of the study.  
339 The authors also thank the J.D. Kline water supply plant authority, Nova Scotia, Canada for  
340 providing access to conduct sample collections in the hydraulic flocculation tanks.

## 341 9. Bibliographic references & notes

- 342 1. J. K. Edzwald, *Water Science and Technology*, 1993, **27**, 21-35.
- 343
- 344 2. J. M. Duan and J. Gregory, *Advances in Colloid and Interface Science*, 2003, **100**, 475-  
345 502.
- 346
- 347 3. J. Bridgeman, B. Jefferson and S. Parsons, *Chemical Engineering Research & Design*,  
348 2008, **86**, 941-950.
- 349
- 350 4. S. H. Kim, B. H. Moon and H. I. Lee, *Microchemical Journal*, 2001, **68**, 197-203.
- 351
- 352 5. R. D. Letterman, A. Amirtharajah and C. R. O'Melia, *Coagulation and flocculation.*,  
353 American Water Works Association, McGraw Hill, New York, 5<sup>th</sup> edn., 1999.
- 354
- 355 6. I. G. Droppo, G. G. Leppard, D. T. Flannigan and S. N. Liss, *Water Air and Soil*  
356 *Pollution*, 1997, **99**, 43-53.
- 357
- 358 7. AWWA, *Operational control of coagulation and filtration processes*, American Water  
359 Works Association, Denver, CO, 2<sup>nd</sup> edn., 2000.
- 360
- 361 8. AWWA and ASCE, *Mixing, coagulation, and flocculation.*, McGraw Hill, American  
362 Water Works Association and American Society of Civil Engineering, New York,  
363 5<sup>th</sup> edn., 2012.
- 364
- 365 9. M. Pivokonsky, P. Bubakova, L. Pivokonska and P. Hnatukova, *Environmental*  
366 *Technology*, 2011, **32**, 1355-1366.

- 367  
368 10. B. Gorczyca and J. Ganczarzyk, *Water Quality Research Journal of Canada*, 1999, **34**,  
369 653-666.  
370  
371 11. A. J. Manning and K. R. Dyer, *Marine Geology*, 1999, **160**, 147-170.  
372  
373 12. Y. S. Vadasarukkai, G. A. Gagnon, D. R. Campbell and S. C. Clark, *Journal American*  
374 *Water Works Association*, 2011, **103**, 66-80.  
375  
376 13. D. C. Hopkins and J. J. Ducoste, *Journal of Colloid and Interface Science*, 2003, **264**,  
377 184-194.  
378  
379 14. K. Samaras, A. Zouboulis, T. Karapantsios and M. Kostoglou, *Chemical Engineering*  
380 *Journal*, 2010, **162**, 208-216.  
381  
382 15. M. C. Kavanaugh and J. O. Leckie, *Particulates in water: characterization, fate, effects,*  
383 *and removal.*, American Chemical Society, Washington D.C., 1980.  
384  
385 16. B. Gorczyca and J. Ganczarzyk, *Environmental Technology*, 1996, **17**, 1361-1369.  
386  
387 17. B. Gorczyca and P. Klassen, *Water Quality Research Journal of Canada*, 2008, **43**, 239-  
388 247.  
389  
390 18. D. H. Li and J. Ganczarzyk, *Research Journal of the Water Pollution Control*  
391 *Federation*, 1991, **63**, 806-814.  
392  
393 19. P. Jarvis, B. Jefferson and S. Parsons, *Water Science and Technology*, 2004, **50**, 63-70.  
394  
395 20. M. A. Yukselen and J. Gregory, *International Journal of Mineral Processing*, 2004, **73**,  
396 251-259.  
397  
398 21. R. J. Gibbs and L. N. Konwar, *Environmental Science & Technology*, 1982, **16**, 119-121.  
399  
400 22. A. L. de Oliveira, P. Moreno, P. A. G. da Silva, M. De Julio and R. B. Moruzzi,  
401 *Desalination and Water Treatment*, 2015, 1-12.  
402  
403 23. R. K. Chakraborti, J. F. Atkinson and J. E. Van Benschoten, *Environmental Science &*  
404 *Technology*, 2000, **34**, 3969-3976.  
405  
406 24. J. Garcia-Sucerquia, W. B. Xu, S. K. Jericho, P. Klages, M. H. Jericho and H. J. Kreuzer,  
407 *Applied Optics*, 2006, **45**, 836-850.  
408  
409 25. J. Sheng, E. Malkiel and J. Katz, *Applied Optics*, 2006, **45**, 3893-3901.  
410  
411 26. A. K. Stoddart and G. A. Gagnon, *Journal American Water Works Association*, 2015,  
412 **107**, E638-E647.

- 413  
414 27. K. Nakamura, H. J. Kreuzer and A. Wierzbicki, *Quantum Control and Measurement*,  
415 1993, 271-276.  
416  
417 28. D. L. Marchisio, R. D. Vigil and R. O. Fox, *Chemical Engineering Science*, 2003, **58**,  
418 3337-3351.  
419  
420 29. O. P. Prat and J. J. Ducoste, *Chemical Engineering Science*, 2006, **61**, 75-86.  
421  
422 30. P. G. Saffman and J. S. Turner, *Journal of Fluid Mechanics*, 1956, **1**, 16-30.  
423  
424 31. J. Abrahamson, *Chemical Engineering Science*, 1975, **30**, 1371-1379.  
425  
426 32. H. H. Ngo, S. Vigneswaran and H. B. Dharmappa, *Environmental Technology*, 1995, **16**,  
427 55-63.  
428  
429 33. J. Gregory, *Filtration & Separation*, 1998, **35**, 367-371.  
430

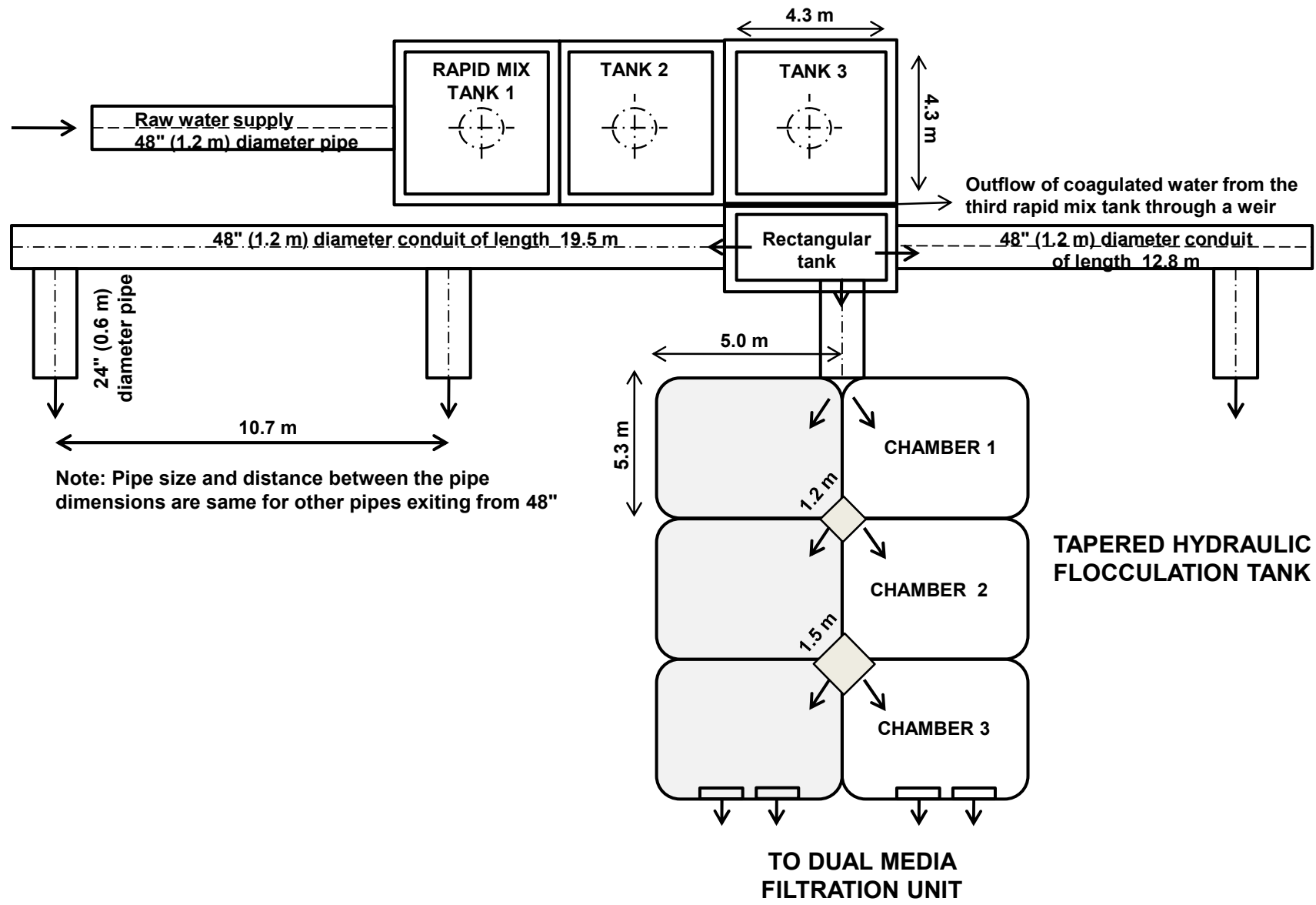


Fig. 1 Schematic overview of the treatment processes of a direct filtration system at the J.D. Kline Water Supply Plant (Halifax, Canada) (adapted from Vadasarukkai et al.<sup>9</sup>).  
Note: Not to scale

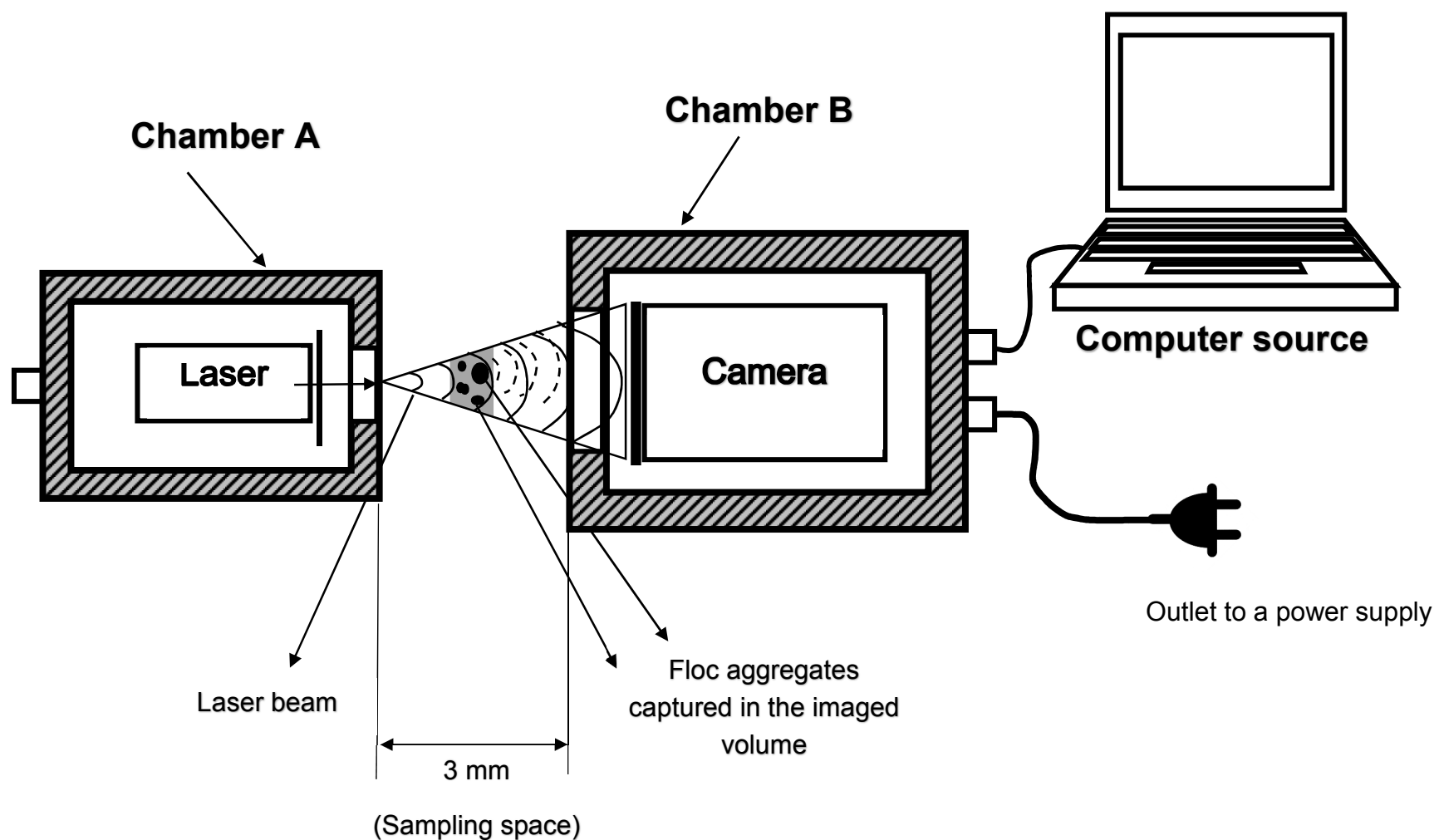


Fig. 2 A schematic diagram of a submersible digital inline holographic microscope (DIHM). Two pressure chambers-A & B, a 365 nm laser light source, imaged volume, camera sensor, and computer source are shown.

Note: Not to scale

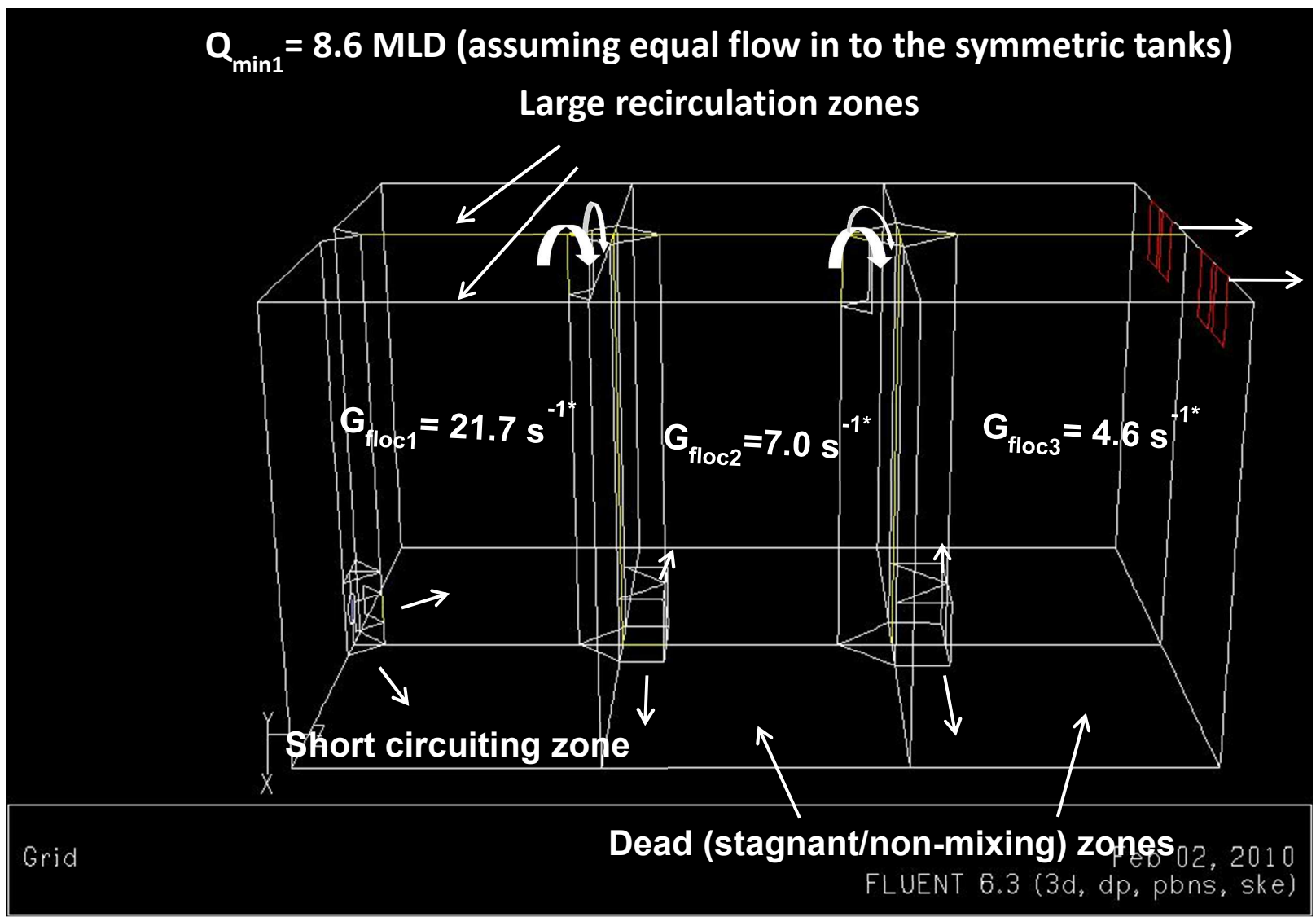


Fig. 3 A three dimensional geometry of the three-stage tapered hydraulic flocculation tank along with the flow characteristics.

$G_{\text{floc}1}$ ,  $G_{\text{floc}2}$ ,  $G_{\text{floc}3}$ - the average velocity gradient in the first, second and third flocculation chambers, respectively.

\* The average G-value was 21.7, 7 and 4.6  $\text{s}^{-1}$  in the first, second and third flocculation chambers at a plant flow of 90 MLD was computed from the numerical analysis (Vadasarukkai et al.<sup>9</sup>).

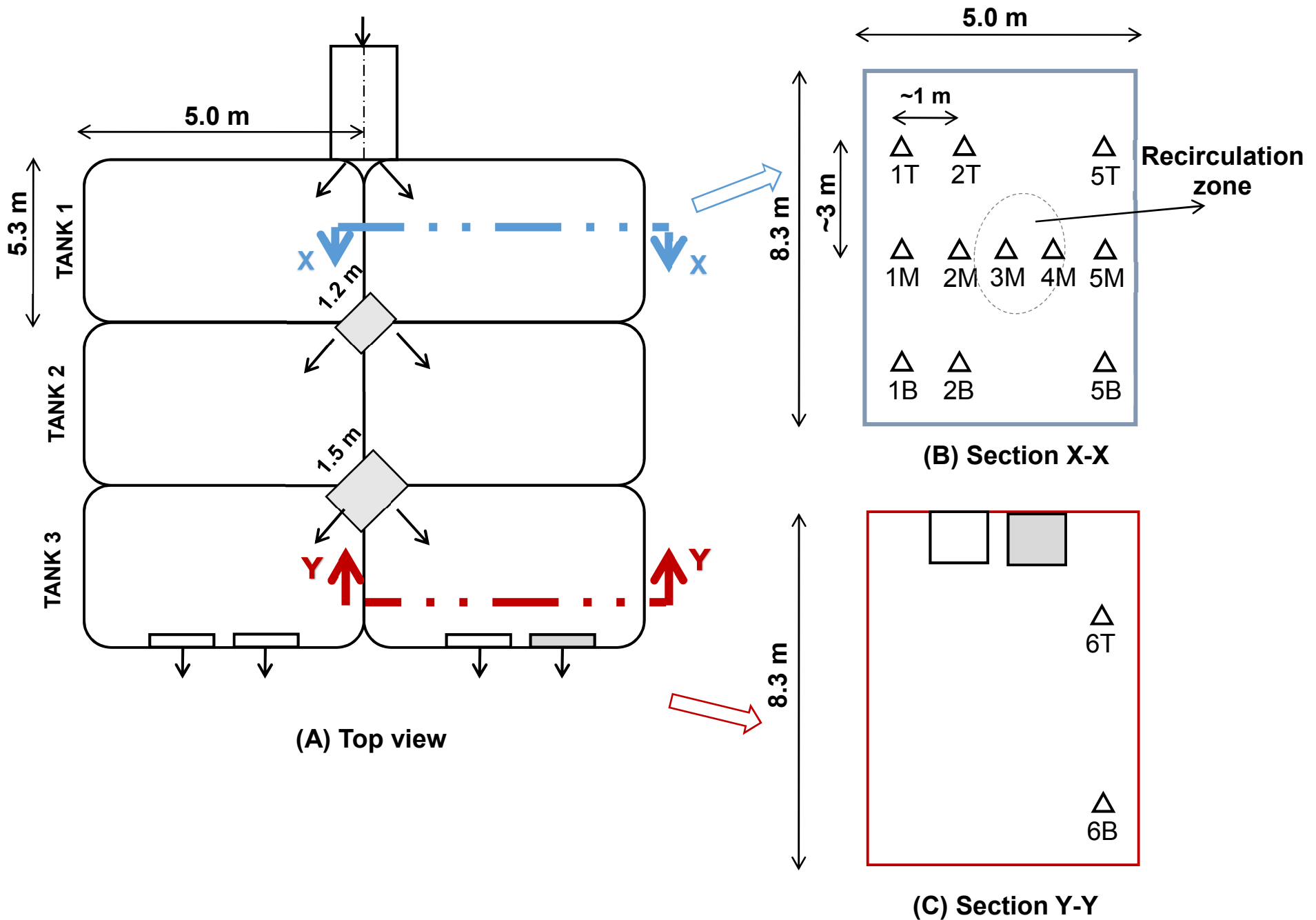


Fig. 4 Thirteen sampling locations selected in one parallel set of a flocculation tank for the digital inline holographic microscope (DIHM) analysis- (A) top view of the entire tank (B) sectional view X-X of chamber-1 and (C) sectional view Y-Y of chamber-3.

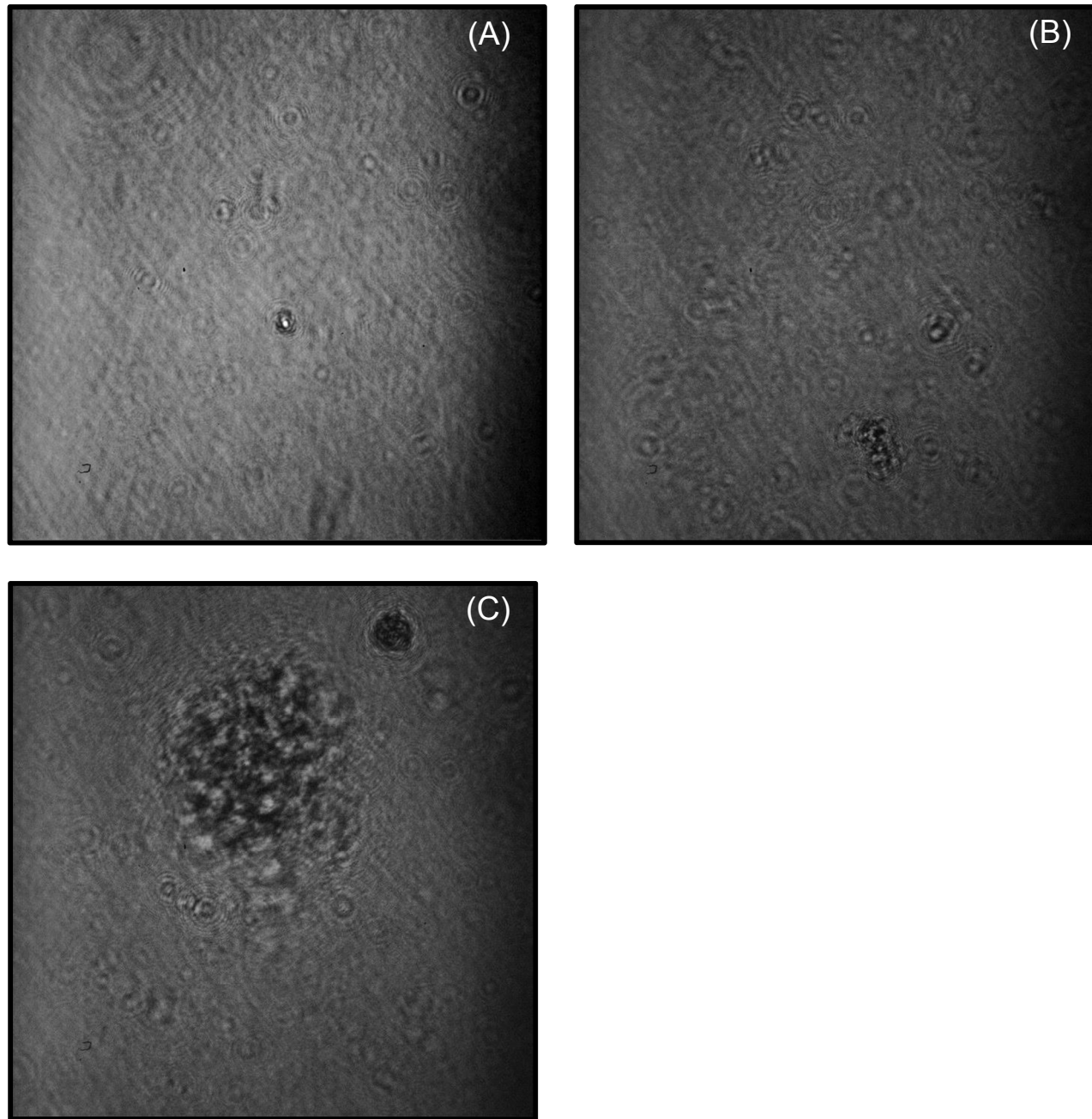


Fig. 5 Illustration of holograms recorded at (A) 1B, (B) 1M and (C) 1T locations using the DIHM technique.  
Note: Scale: 100 nm

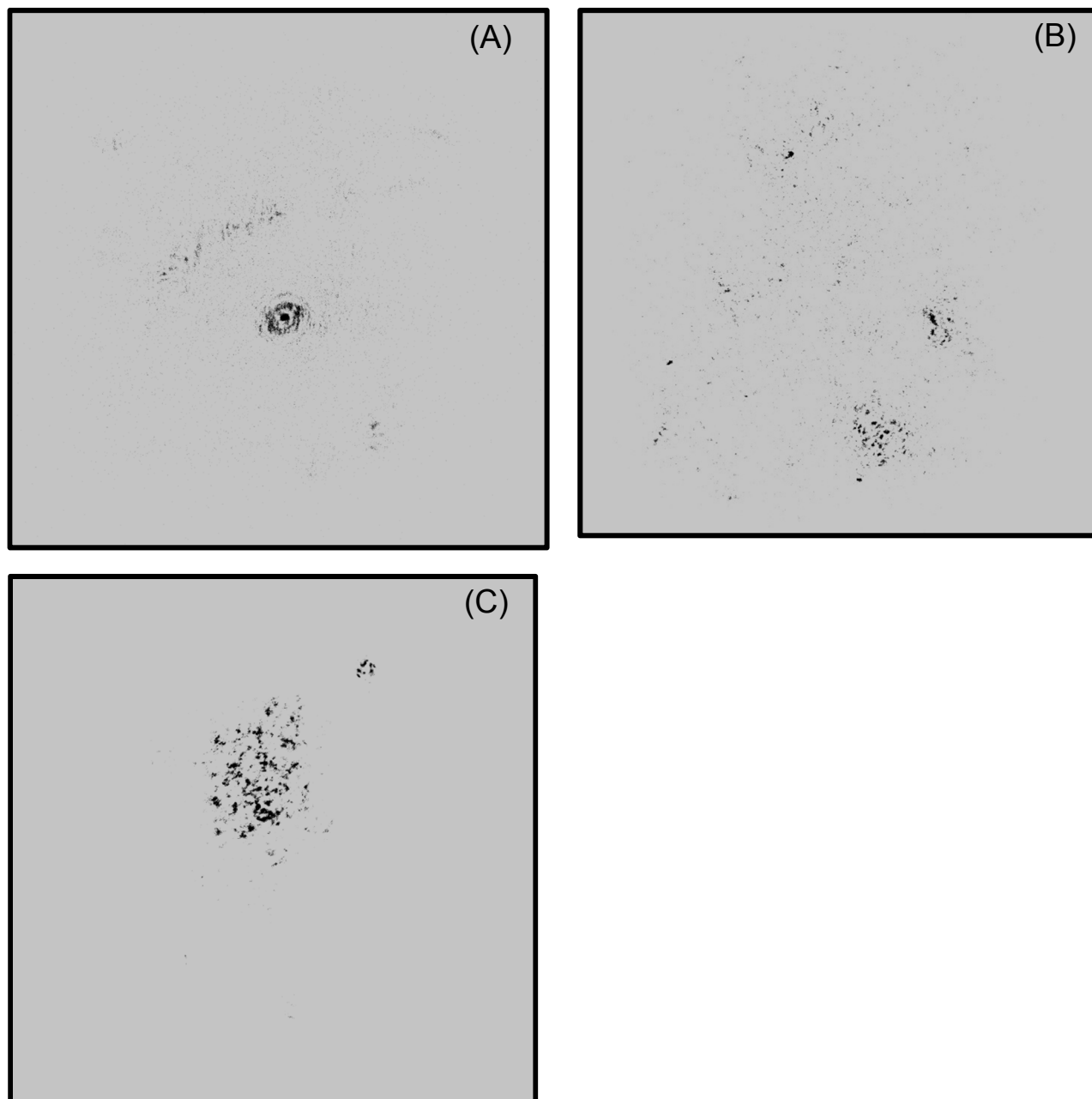


Fig. 6 Example of reconstruction step- a difference hologram reconstructed after subtracting the background noise from consecutive hologram pairs at locations 1B, 1M and 1T. (Scale: 100 nm)

Note: Flocs appear as dark spots on the lighter background, the background was changed to a lighter color for better visibility.

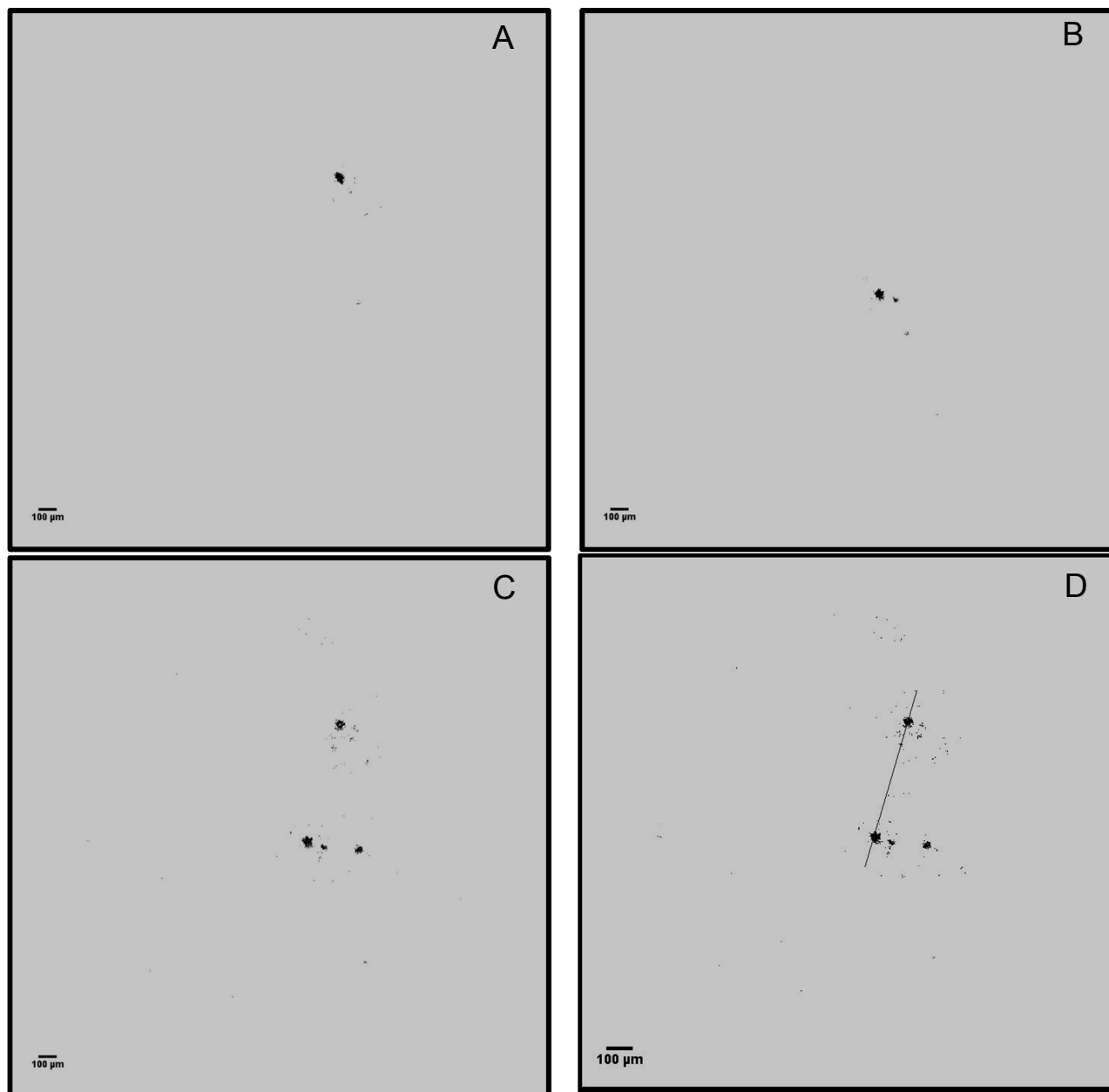


Fig. 7 Illustration of the relative floc velocity measurement- (A-B) trajectories of a floc aggregate captured using two successive reconstructed holograms (C) superimposing of the two reconstructed holograms to obtain the path travelled by a floc aggregate (D) measurement of the distance travelled. (Scale: 100 nm)

Note: Floccs appear as dark spots on the lighter background, the background was changed to a lighter color for better visibility.

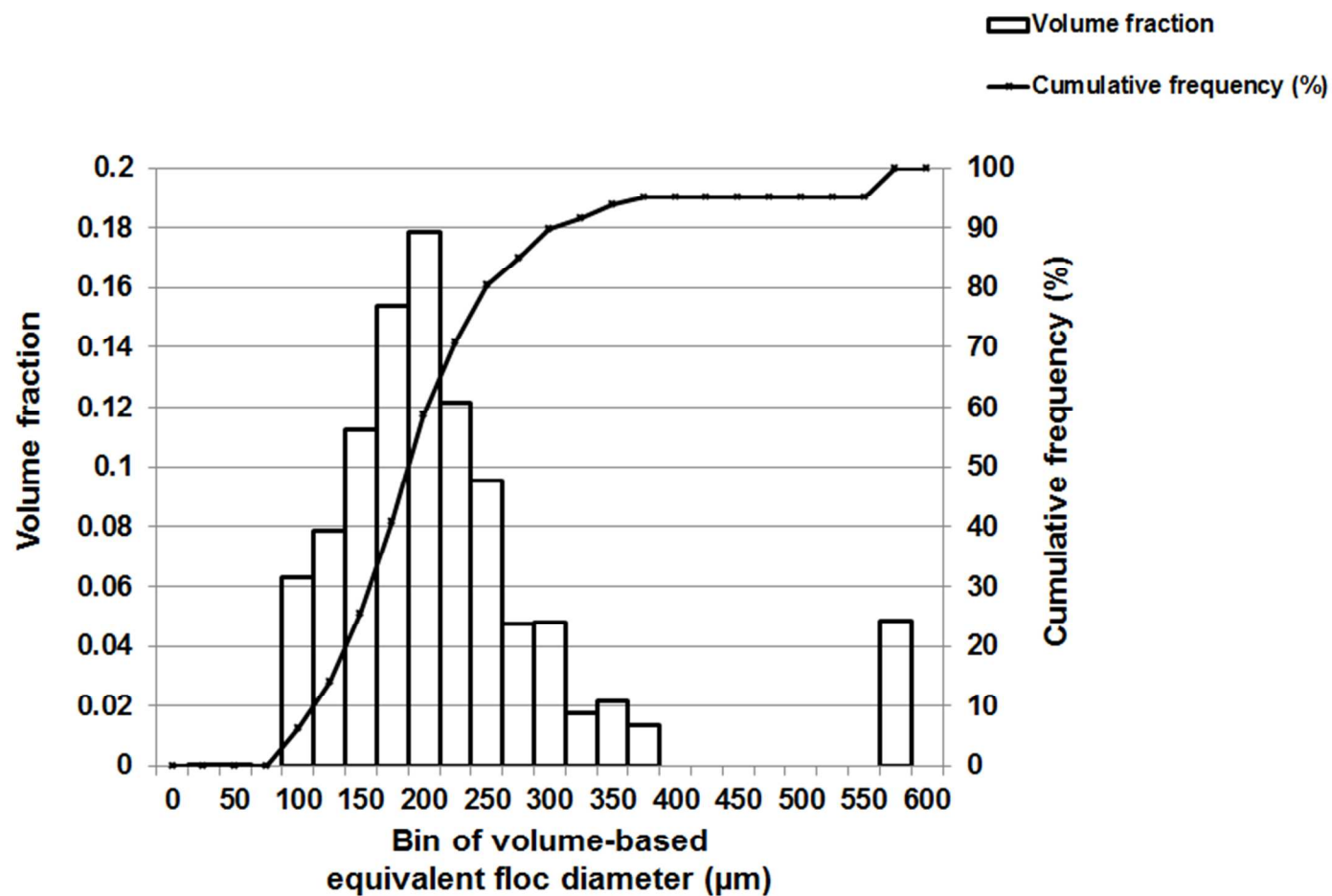
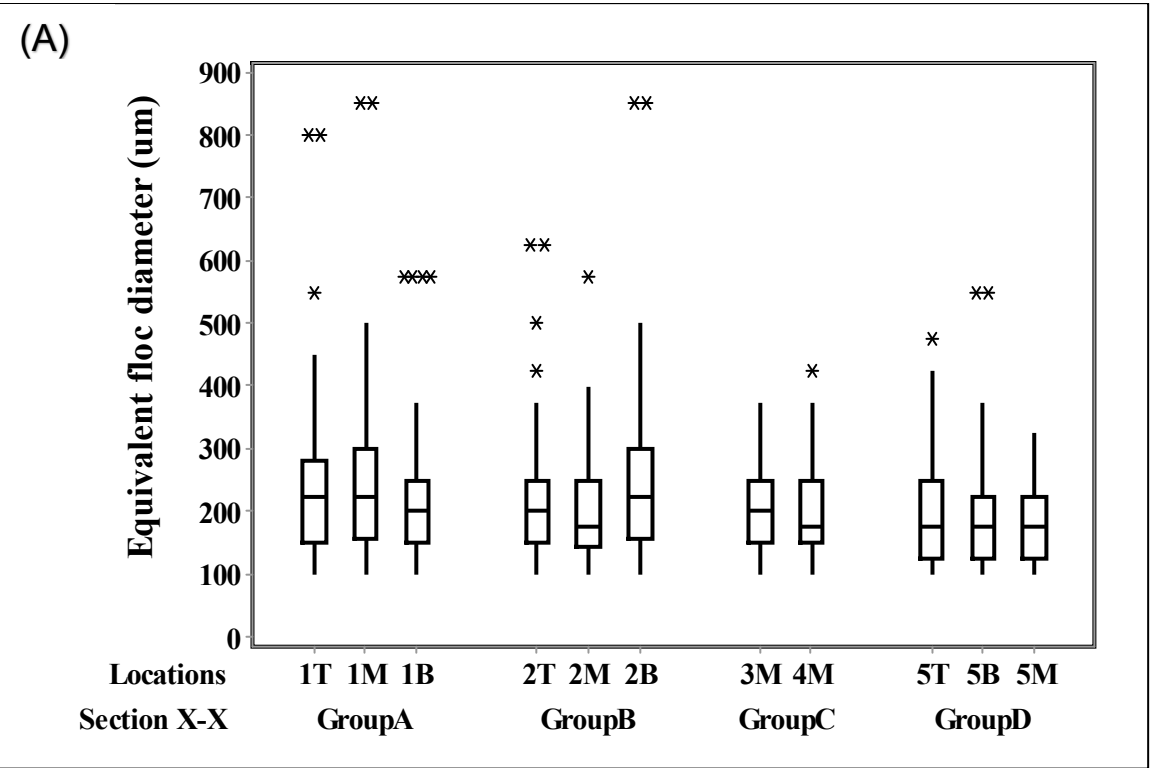


Fig. 8 Illustration of the floc size distribution (by volume) with a total floc count of 830 flocs was calculated at the location, 1B, in the flocculation chamber-1.



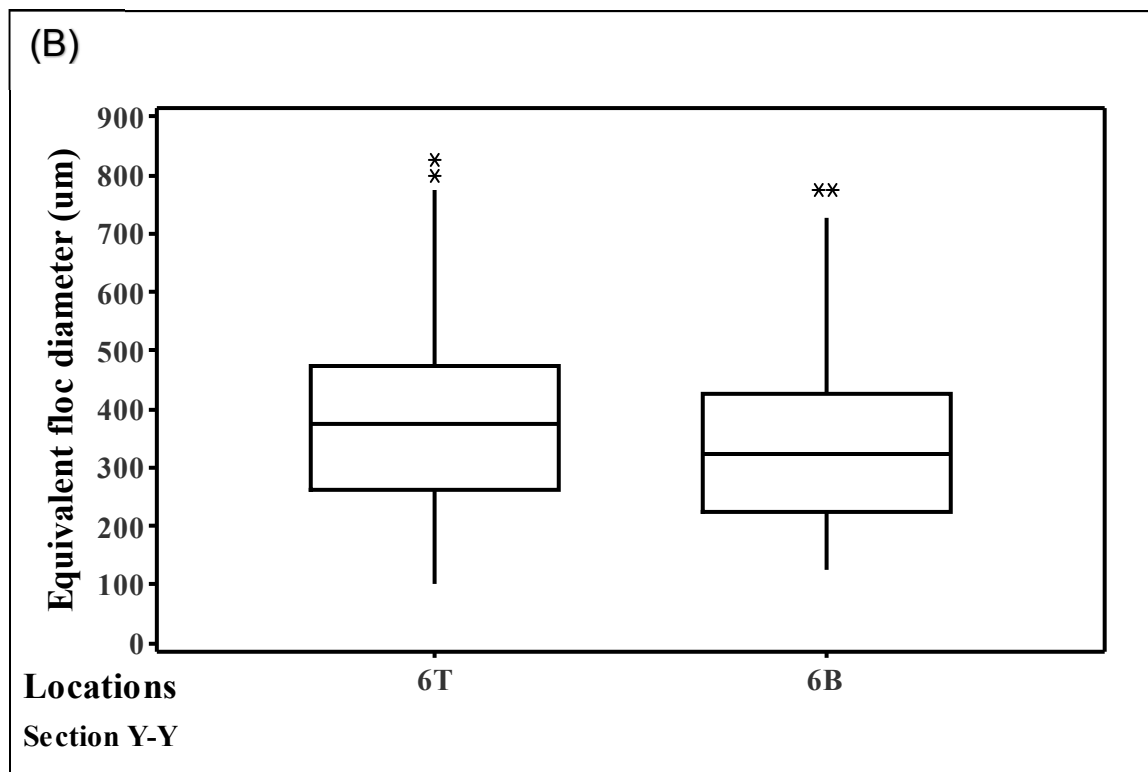


Fig. 9 Box and whisker plots of the spatial distribution of the volume-based floc equivalent diameter measured at different floc monitoring stations- (A) represents floc sizes formed in chamber-1 and (B) represents floc distribution in chamber-3.

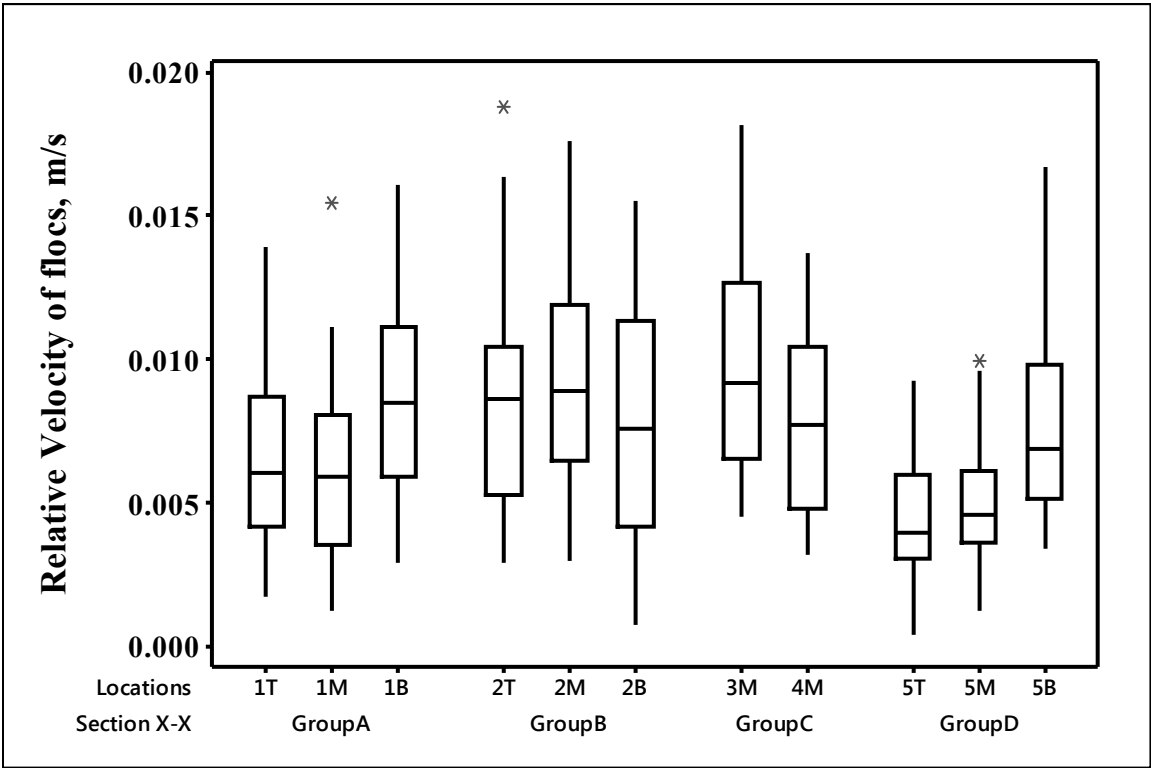


Fig. 10 Box and whisker plots of the relative velocities of flocs with respect to the fluid motion calculated at the sampling locations in the flocculation chamber-1.